Modeling and numerical calculation of waterflooding using the Weierstrass elliptic functions

Vladimir I. Astafev and Andrey E. Kasatkin

***Abstract* —** Waterflooding is the most commonly used *secondary oil recovery method* for both conventional and heavy oil reservoirs because of its relative simplicity, availability of water and cost-effectiveness. The recovery factor for waterflooding is determined by much number of external factors, including number and placement of water injection and oil production wells. The choice of these parameters to maximize the reservoir sweep is the first step of waterflooding optimization and an essential part of the oil field development modeling.

The water injection and oil production wells are usually placed as some periodic array of wells. A five-spot pattern is often the most effective type of waterflooding. Some other patterns are four-spot, seven-spot, nine-spot, direct-line drive, staggered-line drive and so one. All these patterns may be considered as elements of an unbounded double periodic array of wells. Prediction of the motion of the oil-water contact boundary has great importance in the problems of design of oilfield development by waterflooding: knowledge of the nature of coupled motion of oil and water, displacing oil in the reservoir allows us to optimize the system of oil field development.

The simplest model of coupled filtering of oil and water is the model of "multicolored" liquids, which assumes that oil and water have the same or similar physical properties (density and viscosity). A more complex "piston-like" model of oil-water displacement takes into account differences in viscosity and density of the two fluids. Oil reservoir assumed to be homogeneous and infinite, fixed thickness, with constant values of porosity and permeability coefficients. It is assumed that the reservoir is developed by a group of a finite number of production and injection wells recurrent in two directions (doubly-periodic cluster). Filtration of liquids is described by Darcy's law. It is assumed, that both fluids are weakly compressible and the pressure in the reservoir satisfies the quasi-stationary diffusion equation.

Piston-like displacement model leads to the discontinuity of the tangential component of the velocity vector at the boundary of oil-water contact. Use of the theory of elliptic functions in conjunction with the generalized Cauchy integrals reduces the problem of finding the current boundaries of oil-water contact to the system of singular integral equations for the tangential and normal components of the velocity vector and the Cauchy problem for the integration of the differential equations of motion of the boundary of oil-water contact.

***Keywords* —** Weierstrass elliptic functions, Waterflooding, Mathematical modelling, Numerical solution.

This paper is supported by Russian Science Foundation under Grant 15-17-00019 and is based on the abstract, prepared to WSEAS International Conference on Applied and Computational Mathematics (ICACM'15), Seoul, Korea, September 5-7, 2015.

Vladimir I. Astafev was with Samara State University, Continuum Mechanics Department, Samara 443011, Russia. He is now with Samara State Technical University, Oil Field Development Department, Samara 443100, Russia (corresponding author to provide phone / fax: + 7 – 846 – 279 - 0364; e-mail: vladimir.astafev@mail.ru).

Andrey E. Kasatkin is with Samara State University, Samara 443011, Russia (e-mail: darantion_yar@mail.ru).

I. Introduction

Weierstrass elliptic functions (single-valued doubly periodic functions of the complex variable $z = x + iy$, the only singularities on the complex z-plane are poles) are widely used in various applications of mechanics and physics. In solids mechanics elliptic functions are widely used for perforated plates and shells or plates and shells with a doubly periodic system of cracks [1-5] as well as in studies of screw dislocations motion in crystals [6]. In aero- and hydrodynamics, elliptic functions are used to describe the fluid flow through doubly periodic lattice profiles [7], the motion of doubly periodic systems of point vortices [8-10].

Unfortunately, the researches on the water flooding started in the 60s years of the 20th century by H.J. Morel-Seitoux [11] and by R.T. Fazlyev [12] are not well developed. Therefore the purpose of the present work is to open the way to use the Weierstrass elliptic functions in the oil industry. As this takes place, doubly periodic systems of oil wells have been selected as the object for the utilization of such functions. The previous paper by V.I. Astafev and P.V. Roters [13] has considered the case of oil field development by doubly periodic system of production wells. Simulation of the oil field waterflooding via the Weierstrass elliptic functions is the main objective of the proposed research.

II. Weierstrass Elliptic Functions

The main elliptic function is the Weierstrass *P*-function. It can be represented as follows [14-15]:

$$P(z) = \frac{1}{z^2} + \sum_{m,n=-\infty}^{\infty}{}' \left\{ \frac{1}{(z-\omega)^2} - \frac{1}{\omega^2} \right\}, \qquad (1)$$

where $\omega = m\omega_1 + n\omega_2$ $(m, n = 0, \pm1, \pm2, ...)$ are the nodes of the period lattice Ω (Fig. 1). The prime in the sum (1) means that the summation is extended over all pairs of m and n, except m=n=0.

The *P*-function defined in (1) has second-order poles at all nodes of the periodic lattice. The main property of the *P*-function is its double periodicity

$$\left.\begin{aligned} P(z+\omega_1) &= P(z) \\ P(z+\omega_2) &= P(z) \end{aligned}\right\}, \tag{2}$$

where ω_1 and ω_2 are the periods of the Weierstrass *P*-function. The derivatives of the *P*-function are also doubly periodic, and any elliptic function can be represented as a linear combination of the *P*-function and its derivatives.

Integration of the *P*-function (1) can be written as [14-15]:

$$\zeta(z) = -\int P(z)dz = \frac{1}{z} + \sum_{m,n=-\infty}^{\infty}{}'\{\frac{1}{z-\omega} + \frac{1}{\omega} + \frac{z}{\omega^2}\}, \tag{3}$$

where $\zeta(z)$ is the Weierstrass zeta-function.

Integration of the zeta-function (3) leads to the Weierstrass sigma-function $\sigma(z)$ [14-15]:

$$\ln\sigma(z) = \ln z + \sum_{m,n=-\infty}^{\infty}{}'\left\{\ln(\frac{z-\omega}{\omega}) + \frac{z}{\omega} + \frac{z^2}{2\omega^2}\right\}. \tag{4}$$

In contrast to $P(z)$, functions $\zeta(z)$ and $\sigma(z)$ do not possess the property of double periodicity. Instead of (2), they satisfy the following conditions of quasi-periodicity [14-15]:

$$\left.\begin{aligned} \zeta(z+\omega_1) &= \zeta(z) + 2\eta_1 \\ \zeta(z+\omega_2) &= \zeta(z) + 2\eta_2 \end{aligned}\right\}, \tag{5}$$

$$\left.\begin{aligned} \ln\sigma(z+\omega_1) &= \ln\sigma(z) + \eta_1(2z-\omega_1) \\ \ln\sigma(z+\omega_2) &= \ln\sigma(z) + \eta_2(2z-\omega_2) \end{aligned}\right\}, \tag{6}$$

where $\eta_1 = \zeta(\omega_1/2)$, and $\eta_2 = \zeta(\omega_2/2)$.

The values η_1, η_2, ω_1 and ω_2 are not independent but related by the Legendre identity [14-15]:

$$\eta_1\omega_2 - \eta_2\omega_1 = \pi i. \tag{7}$$

The values of the lattice periods ω_1 and ω_2 can be arbitrary complex numbers with the main restriction as $Im(\omega_2/\omega_1) > 0$. This lattice Ω and its base element, which is called as the fundamental parallelogram of periods, are shown in Fig. 1.

The fundamental parallelogram constructed on the basis of ω_1 and ω_2 has the following main parameters (Fig. 1):

$$\tau = \omega_2/\omega_1 = \lambda e^{i\theta} \quad \Delta = \mathrm{Im}(\overline{\omega_1}, \omega_2) = |\omega_1|^2 \lambda \sin\theta$$

Note that pairs (ω_1, ω_2), $(\omega_1+\omega_2, \omega_2)$, $(\omega_2, -\omega_1)$ and $(\omega_1, \omega_2-\omega_1)$ define the same doubly periodic lattice Ω. Therefore, all the variety of lattices Ω can be characterized by a dimensionless parameter τ, changing in a fundamental half-domain (Fig. 2)

$$D'_0 = \{\tau : 0 \le \mathrm{Re}\,\tau \le 1/2, |\tau| \ge 1\}$$

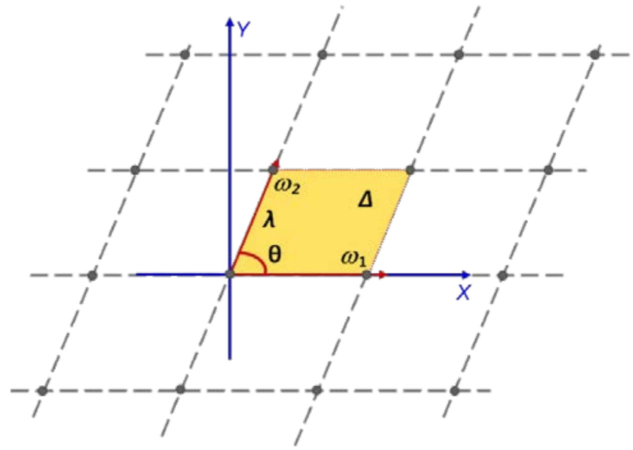

Fig. 1. Doubly periodic lattice Ω with the periods ω_1 and ω_2 and its fundamental parallelogram.

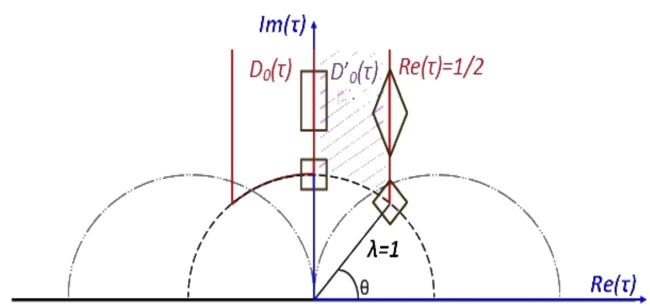

Fig. 2. The fundamental domain D_0 and half-domain D'_0 for the modulus τ

II MATHEMATICAL MODEL

Consider the plane filtration flow of a viscous compressible fluid with viscosity μ and compressibility β in an infinite horizontal reservoir with permeability *k*, porosity *m* and thickness *h*. For the quasi-stationary state of filtration flow the pressure in the reservoir $p(x,y,t)$ satisfies the diffusivity equation and the velocity components $V_x(x,y,t)$ and $V_y(x,y,t)$ are calculated by the Darcy law [16-17]

$$\frac{\partial p}{\partial t} = \chi(\frac{\partial^2 p}{\partial x^2} + \frac{\partial^2 p}{\partial y^2}), \; V_x = -\frac{k}{\mu}\frac{\partial p}{\partial x}, \; V_y = -\frac{k}{\mu}\frac{\partial p}{\partial y}, \tag{8}$$

where $\chi = k/m\mu\beta$ - the coefficient of diffusivity.

Simulated reservoir is developed by a doubly periodic system of production and injection wells. The water injection and oil production wells are usually placed as some periodic array of wells (so-called - four-spot, five-spot, seven-spot, nine-spot, direct-line drive, staggered-line drive patterns and so on). Two examples of these patterns with corresponding fundamental parallelograms of periods are shown on the Fig.3.

Prediction the motion of the oil-from injection to production well as well as the motion the oil-water contact boundary has the great importance in the problems of design of oilfield development by waterflooding:
knowledge of the nature of coupled motion of oil and water, displacing oil in the reservoir allows us to optimize the system of oil field development.

Solution of the equation (8) in the case of doubly periodic system of production and injection wells has been obtained in [18-23]. The distribution of the velocity field has been presented by the Weierstrass zeta-function and written as follows:

$$\overline{V}(z,\overline{z}) = V_x(x,y) - iV_y(x,y) = \\ = -\sum_{k=1}^{n} \frac{Q_k}{2\pi h}(\zeta(z-z_k) + \alpha(z-z_k) - \beta(\overline{z}-\overline{z}_k)), \quad (9)$$

where $\zeta(z)$ - Weierstrass zeta function, z_k - location of the k-th well in the cluster, Q_k - flow rate of the k-th well ($Q_k<0$ for the injection well and $Q_k>0$ for the production well), $\alpha = (\beta\overline{\omega}_1 - 2\varsigma(\omega_1/2))/\omega_1$ and $\beta=\pi/\Delta$.

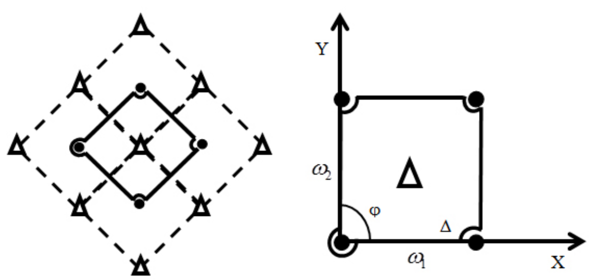

(a)

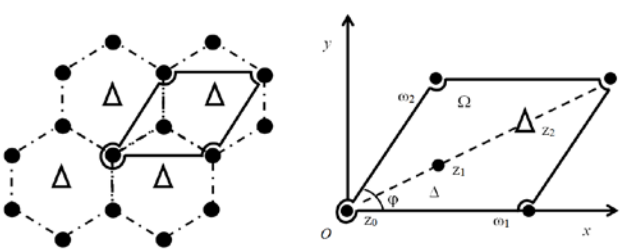

(b)

Fig. 3. Five-spot (a) and seven-spot (b) patterns of flooding (production wells are marked by black circles, injection – by white triangles) and corresponding doubly periodic lattice *Ω*

A Stream Lines

Based on the solution (9), the character of fluid flow (stream lines) from the injection well (marked by ■) to the production wells (marked by ●) for five-spot, seven-spot, nine-spot, and thirteen-spot patterns is shown on the Fig. 4.

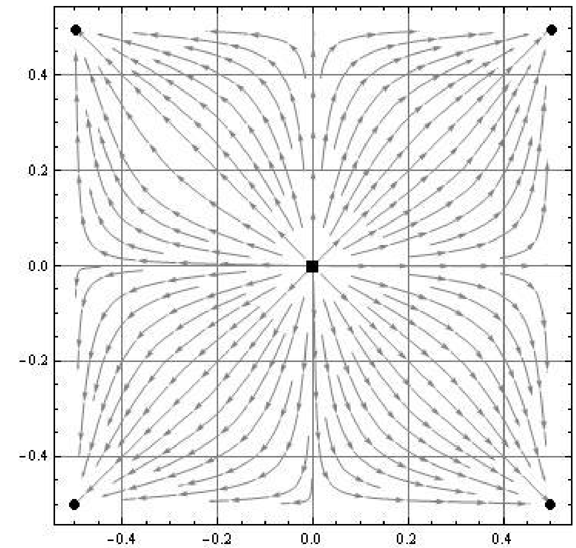

(a)

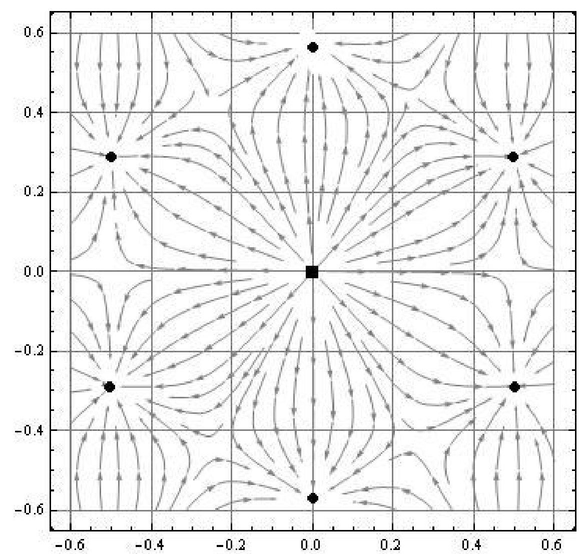

(b)

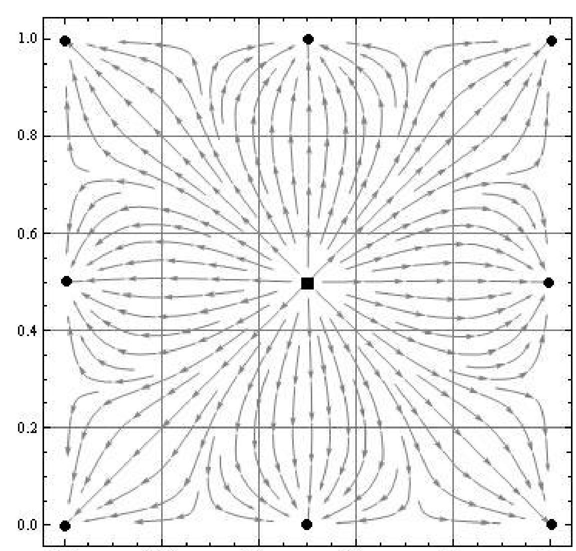

(c)

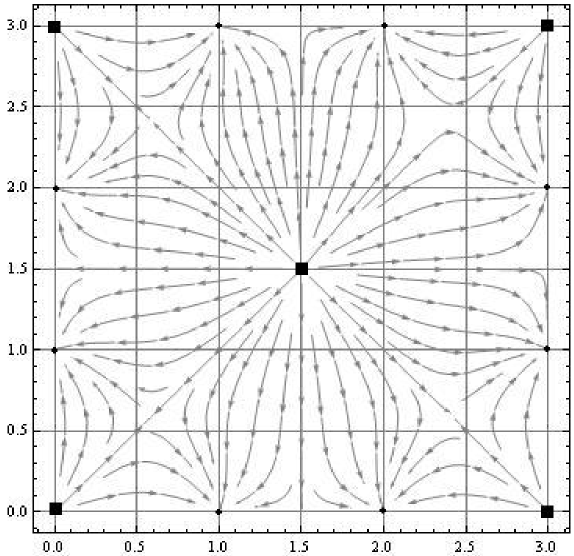

(d)

Fig. 4. The stream lines for five-spot (a), seven-spot (b), nine-spot (c) and thirteen-spot (d) patterns of waterflooding [24].

B Oil-water boundary

To analyze the movement of the oil-water boundary from the injection well to production ones it is necessary to solve the following differential equation in complex variables [20-23]:

$$m\frac{d\bar{z}}{dt}=\bar{V}(z,\bar{z})= \\ -\sum_{k=1}^{n}\frac{Q_k}{2\pi h}(\zeta(z-z_k)+\alpha(z-z_k)-\beta(\bar{z}-\bar{z}_k)), \tag{10}$$

where the initial condition at the time $t=0$ is

$$z(\theta,0)=z_0+r_w e^{i\theta}.$$

Here z_0 is the center of the injection well, r_w is the well radius, m is the porosity of reservoir. To solve the equation (10) with corresponding initial condition, named as the Cauchy problem, we use a Runge-Kutta methods [21-22, modified in response to the complex variables in the equation (10). It should be noted that the solution of the equation (10) is carried out in the dimensionless time $T=mQt/h\left|\omega_1^2\right|$.

Special attention should be paid to the role of the parameter θ. This parameter marks the placement of the water particle $z(\theta, t)$ at the time $t>0$, started at the time $t=0$ from the point $z(\theta, 0)$ and moved to the point $z(\theta, t)$ in accordance with the equation (10). Simply speaking, the solution $z(\theta, t)$ of the equation (10) is the trajectory of the water particle, marked by the parameter θ, from injection well to production one.

Thus, the solution of the equation (10) for different values of parameter $0<\theta<\pi$ is a set of water flow curves or injected water spot that "spread out" in the reservoir over time.

On the Fig. 5-7 the results of calculations for several patterns of waterflooding are shown. Fig. 5-7 show the injected water area, built for the four-spot, five-spot and nine-spot patterns.

The first image corresponds to the stage of flooding before the breakthrough of water into a production wells and the second one – the stage at the time, when there occur the breakthrough of water into a production well.

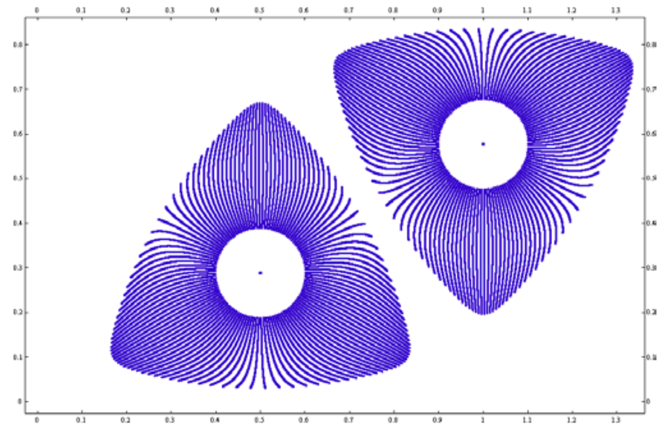

T=500

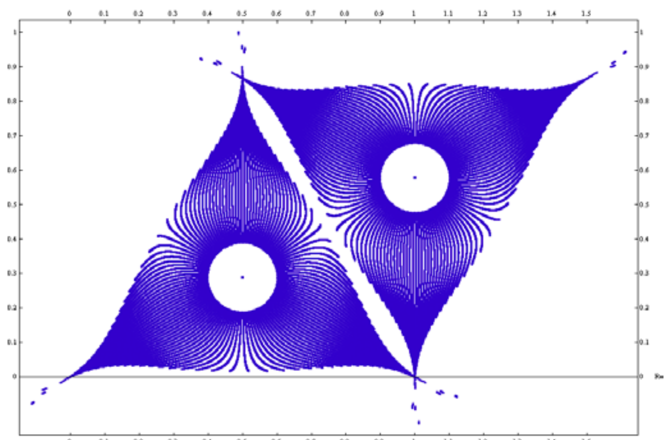

T=700

Fig. 5. The oil-water boundary for the four-spot pattern at time T=500 and T=700.

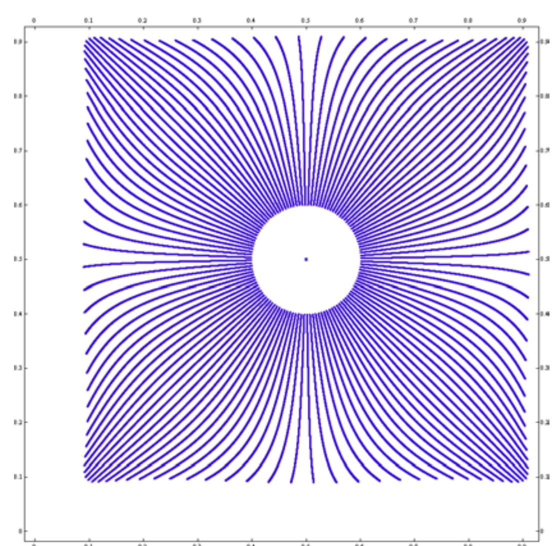

T=1000

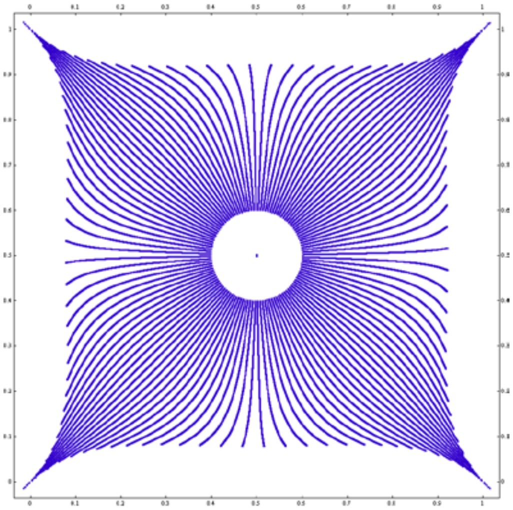

T=1100

Fig. 6. The oil-water boundary for the five-spot pattern at time T=1000 and T=1100.

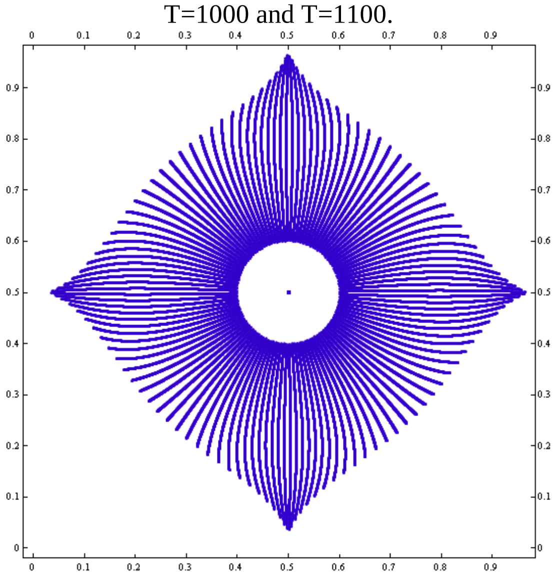

T=450

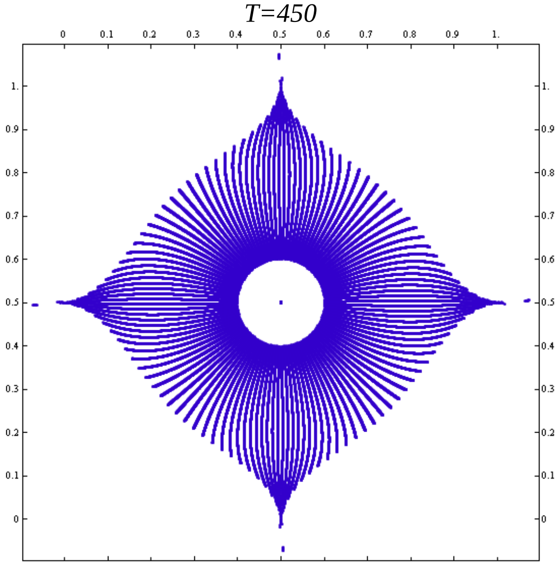

T=465

Fig. 7. The oil-water boundary for the nine-spot pattern at time *T*=450 and T=465.

On the Fig. 8-9 the results of test calculations for one injection and one production well (so- named the Musket problem [16]) are compared with Musket solution. There is a very good correlation of the calculated results with the results of the Muskat [16].

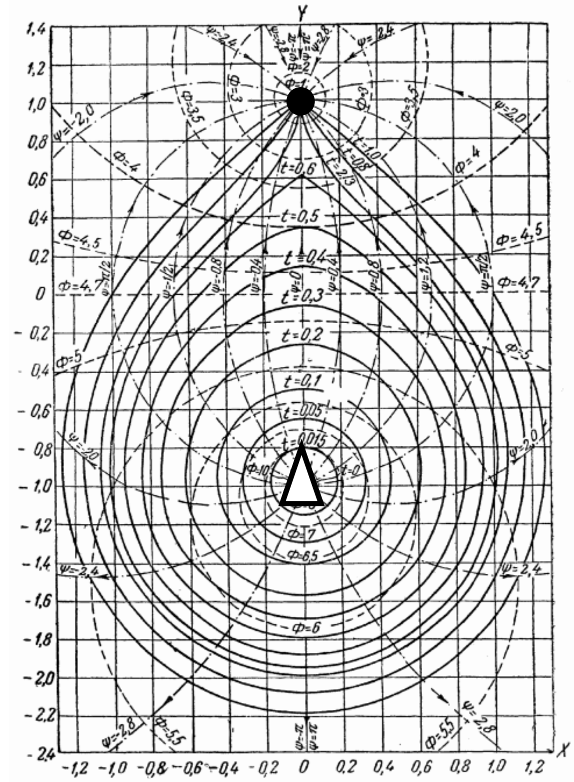

Fig. 8. The oil-water boundary as well the stream lines from injection to production well, calculated by M. Muskat [15]

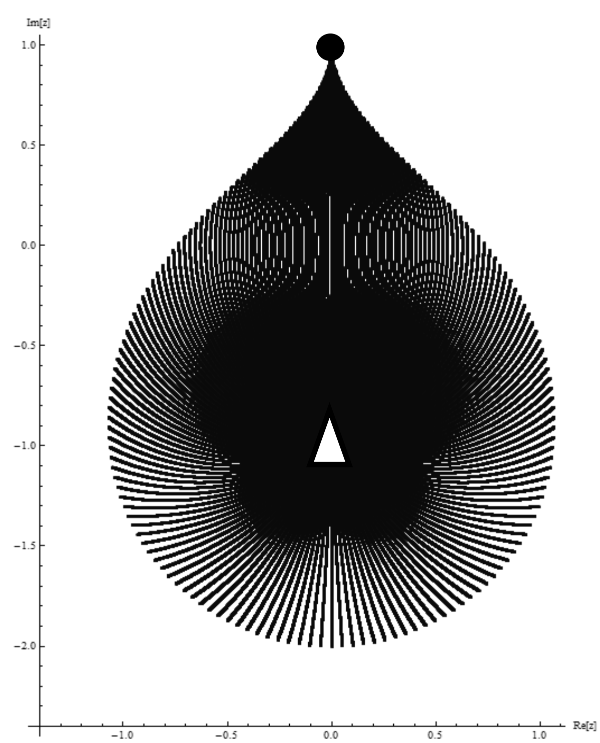

Fig. 9. The oil-water boundary from injection to production well at the time, when the breakthrough of water occurs.

C Piston-like flooding

In the case of the piston-like flooding (moving boundary problem in the theory of filtration) the boundary conditions on the flooding line L (Fig. 10) for the tangential V_t and normal V_n components of the filtration velocity are the follows (the index *o* refers to particles of oil, and the index *w* - to the particles of water) [21-22]:

$$\begin{cases} V_n^{(w)} = V_n^{(o)}; \\ \mu_{(w)} V_t^{(w)} = \mu_{(o)} V_t^{(o)}. \end{cases} \quad (11)$$

Discontinuous on the line L function $V_x(x,y,t) - iV_y(x,y,t)$ on the complex plane $z=x+iy$ will be sought in the following form [21-22]:

$$\begin{aligned} &\overline{V}(z,t) = V_x(x,y,t) - iV_y(x,y,t) = \\ &F(z,t) + \frac{1}{2\pi i}\oint_L \zeta(\tau - z)\gamma(\tau,t)d\tau, \end{aligned} \quad (12)$$

where $F(z,t)$ is given by equation (9).

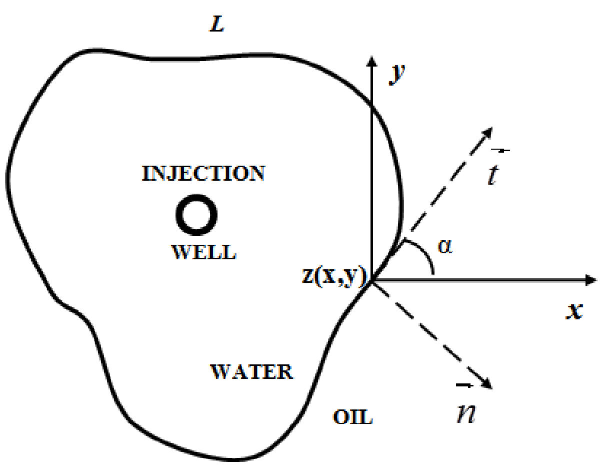

Fig. 10. Line of discontinuity L for the tangential V_t and normal V_n components of the filtration velocity.

Applying the Sokhotsky-Plemel formulas [15], the unknown function $\gamma(s,t)$ and the complex velocity $\overline{V}(z(s))$ at a point $z(s,t)$ of the line L can be expressed as

$$\begin{aligned} &\gamma(s) = \overline{V}^{(w)}(s) - \overline{V}^{(o)}(s), \\ &\overline{V}(s) = (\overline{V}^{(w)}(s) + \overline{V}^{(o)}(s))/2. \end{aligned} \quad (13)$$

Taking into account the boundary conditions (11), the relations (13) can be rewritten as

$$\begin{aligned} &\gamma(s) = (1 - \mu_{(w)}/\mu_{(o)})V_t^{(w)}(s)e^{-i\alpha}, \\ &\overline{V}(s) = ((1 + \mu_{(w)}/\mu_{(o)})V_t^{(w)}(s)/2 + iV_n^{(w)}(s))e^{-i\alpha}, \end{aligned} \quad (14)$$

where α – the angle between the tangent line L and the axis X, i.e. $e^{i\alpha} = dz/ds$ (Fig. 10).

Denoting the viscosity ratio as $\kappa = \mu_{(w)}/\mu_{(o)}$, the normal and tangential velocity components of the water as $T(s) = V_t^{(w)}(s)$ and $N(s) = V_n^{(w)}(s)$, the Eq. (14) allow us to obtain the following singular integral equation for the unknown functions $T(s,t)$ and $N(s,t)$ on the line L:

$$\begin{aligned} &\frac{1+\kappa}{2}T(s,t) + iN(s,t) = \\ &(F(s,t) + \frac{1-\kappa}{2\pi i}\int_0^S \zeta(z(\sigma) - z(s))T(\sigma,t)d\sigma)\frac{dz}{ds}, \end{aligned} \quad (15)$$

The integral equation (15) must be supplemented by a differential equation that determines the time evolution of the line L. This equation has the form [16-17]

$$\begin{aligned} &m\frac{\partial \overline{z}(s,t)}{\partial t} = \overline{V}(z(s,t)), \\ &z(s,0) = z_0 + r_w e^{i\theta}. \end{aligned} \quad (16)$$

where z_0 - the center of the injection well with radius r_w, through which water is pumped into the reservoir. The initial condition (16) indicates the starting position of the point $z(s,0) = z_0 + r_w e^{i\theta}$ in the beginning of flooding, the corresponding angle θ is determined on the contour of the injection well.

Using once more the second Sokhotsky-Plemel formulas and the equation (15), the equation (16) can be rewritten as

$$\begin{aligned} &m\frac{\partial \overline{z(s,t)}}{\partial t}\frac{\partial z}{\partial s} = \frac{(1+\kappa)}{2}T(s,t) + iN(s,t), \\ &z(s,0) = z_0 + r_w e^{i\theta}. \end{aligned} \quad (17)$$

where $T(s)$ and $N(s)$ for a given time t are obtained by solving the singular integral equation (15).

III NUMERICAL SOLUTION

Consider the algorithm for the numerical solution of integral-differential equations (15) and (17). For the numerical solution of singular integral equation (15) we divide the contour L by discrete set of points on the elements $[z_i, z_{i+1}]$, ($i = 0, 1, \ldots N-1$) (Fig. 11).

Due to the closure of line L, the first and the last points of the partition are the same, i.e., $z_N=z_0$. Each of the points z_k corresponds to the length of the arc s_k. Let us choose and fix the point $z_k=z(s_k)$ on the contour L. Separating in equation (15) the real and imaginary parts, we obtain the following equations for the unknown values of $T_k=T(s_k)$ and $N_k=N(s_k)$ at the points $z_k=z(s_k)$:

$$\frac{1+\kappa}{2}T(s_k,t)=\mathrm{Re}\left(\left[F(s_k,t)+\frac{1-\kappa}{2\pi i}\int_0^S \zeta(z(\sigma)-z_k)T(\sigma,t)d\sigma\right]z_k^{'}\right),$$

$$N(s_k,t)=\mathrm{Im}\left(\left[F(s_k,t)+\frac{1-\kappa}{2\pi i}\int_0^S \zeta(z(\sigma)-z_k)T(\sigma,t)d\sigma\right]z_k^{'}\right). \qquad (18)$$

Omitting the rather cumbersome intermediate calculations, we write the approximation of the integral term in equation (18) as follows:

$$\zeta(z(\sigma)-z_k)T(\sigma,t)d\sigma =$$
$$\int_0^S \frac{1}{2z_k^{'}}\left[\begin{array}{l} 2T_k \ln\left(\dfrac{\Delta s_k}{\Delta s_{k-1}}\right)+T_{k-1}-T_{k-1}+ \\ \sum_{i=k+1}^{N+k-1}\zeta(z_i-z_k)T_i(\Delta s_i+\Delta s_{i-1})z_k^{'} \end{array}\right] \qquad (19)$$

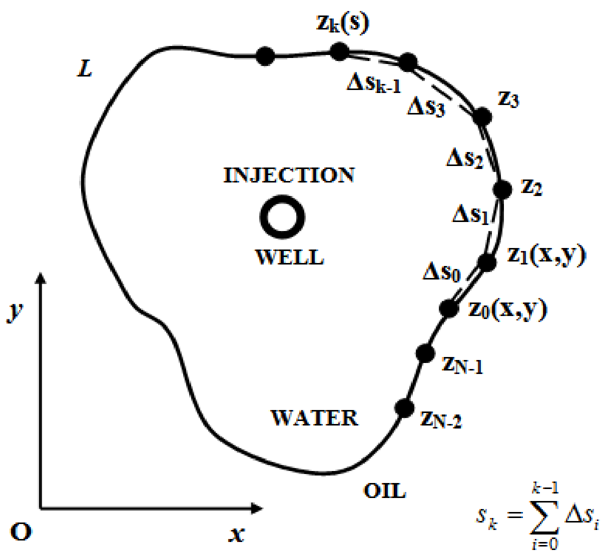

Fig. 11. Parameterization scheme of line L and its discretization by points Z_k $(k=0\ldots N$-`$1)$.

Equations (18) show us that the real part of the singular integral equation (15) matches the finding of values of the unknown function $T_k=T(s_k)$ at a given time t_n on a discrete set of points $z_{k}=z(s_k)$. The imaginary part of this equation is, in fact, the formula for calculating the values of the function $N_k=N(s_k)$ at a given time t_n at the same discrete set of points.

The obtained values of T_k and N_k are then used to calculate the displacements of points $z_{k}=z(s_k)$ in the time interval $[t_n, t_{n+1}]$. These displacements are determined by the numerical solution of the Cauchy problem (17) with the Runge-Kutta method, modified in view of the complex nature of the differential equation (7). In the calculations was chosen the dimensionless time τ, associated with the original time t as

$$\tau = 10^{-4}Qt/2\pi mh\omega_1^2.$$

IV RESULTS OF CALCULATIONS

To solve this problem there was developed software system to track the evolution of the flooding front (line L) in time, as well as to quantify the effectiveness of a particular scheme of flooding (dimensionless water breakthrough time into the production wells τ and waterflooding coverages K_{cov}). In numerical calculations there was considered frontal row, four-point, five-point, seven-point and nine-point scheme of flooding. To determine the current position of the flooding front it was involved 180 tracers - points coming out at the initial time of the injection well.

It is known [24] that the viscosity ratio κ has a negative impact on the ultimate recovery: the decrease in the parameter κ leads to the decrease in the volume of recoverable oil due to the growing instability of oil displacement by water. In addition, when viscosity ratio $\kappa<1$, the Saffman-Taylor instability [25] occurs, which is often called as "viscous fingering".

The viscous fingering effect was observed in the course of our numerical calculations. The fig. 12 shows the formation of viscous fingers for five-point scheme of flooding at $\kappa=1/5$ and $\tau=0.045$ values. For comparison, the fig.12 is supplemented by the figure from [26] (fig. 6a in the cited paper) obtained experimentally for similar geometry placement of wells.

Additionally, the fig. 13a shows us the flooding area for the five-point scheme of flooding and different value of viscosity ratio κ-1/2. For comparison on the fig. 13b it is presented the experimental data from [26].

And finally, on the figs. 14 and 15 it is shown the flooding areas for the seven-point and nine-point schemes of flooding. For comparison the figs. 14a and 15a show the flooding area with viscosity ratio $\kappa=1$ and the fig. 14b and 15b – with $\kappa=1/4$.

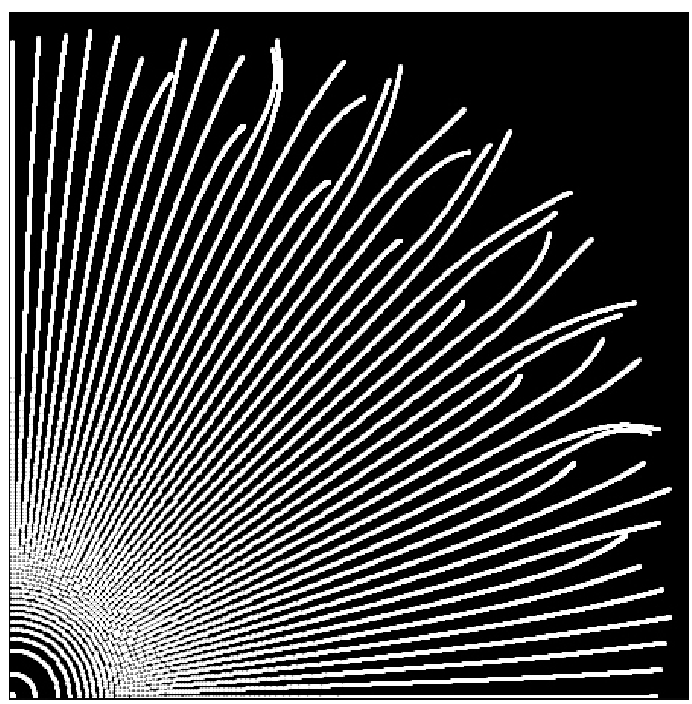

(a)

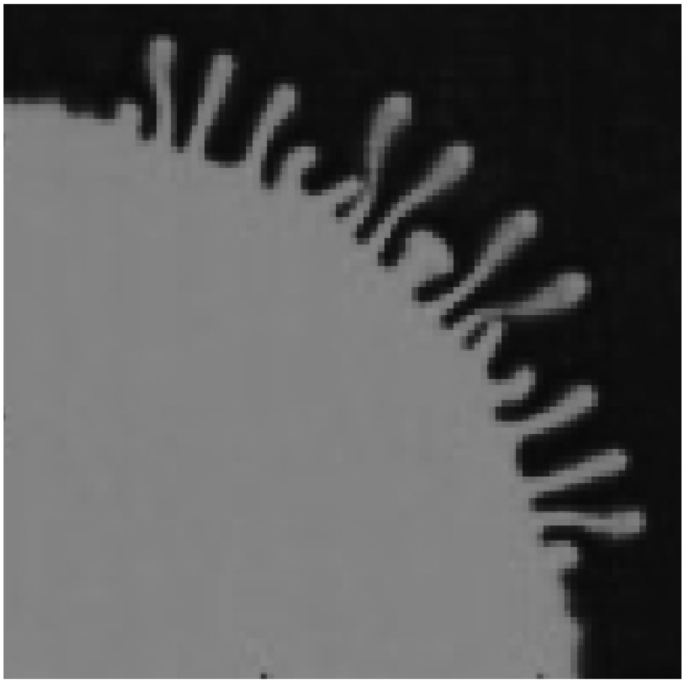

(b)

Fig. 12. Saffman-Taylor instability of the front of flooding for the five-point scheme.

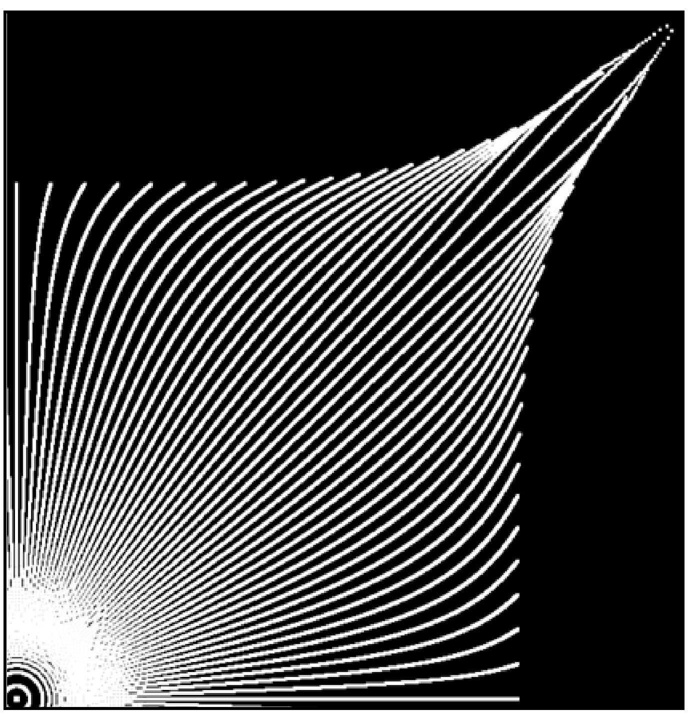

(a)

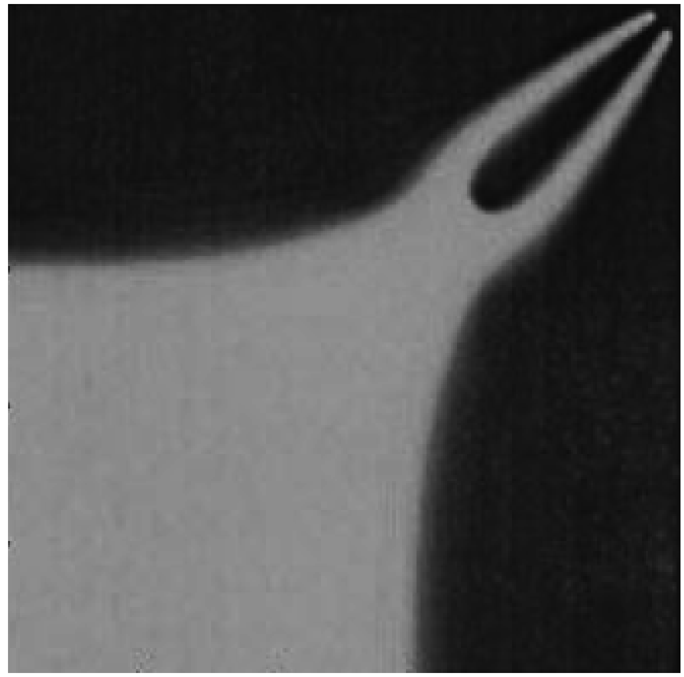

(b)

Fig. 13. Saffman-Taylor instability near the producing well for the five-point scheme. The numerical calculation for the mobility κ=1/2 and τ = 0.096 (a), the data from [26] (b).

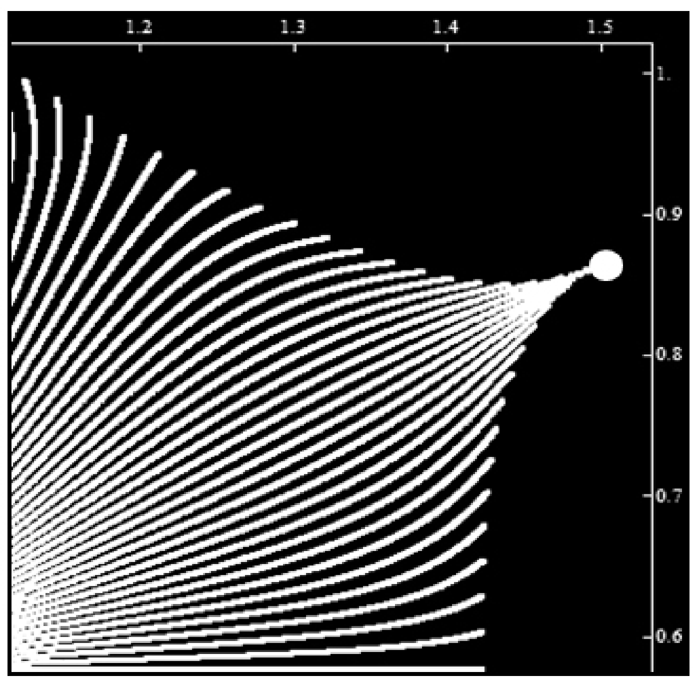

(a)

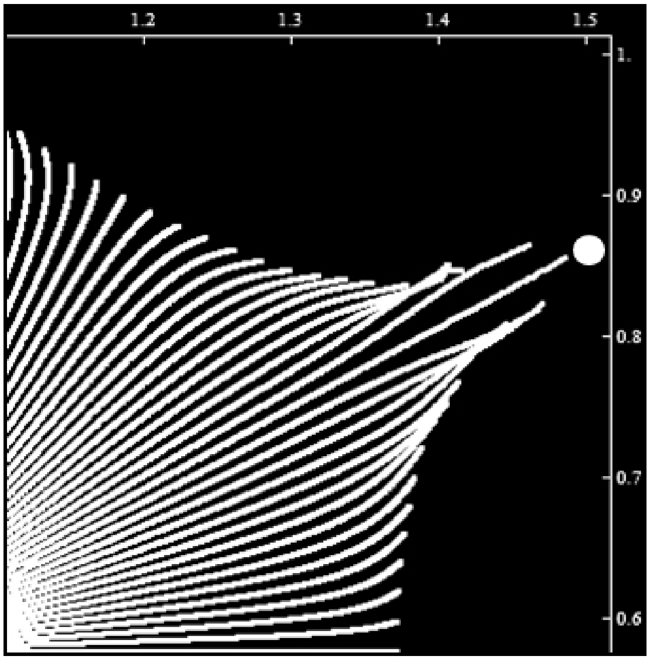

(b)

Fig. 14. The flooding area for seven-point scheme of flooding for κ=1 and τ=0.0516 (a); for κ=1/4 and τ=0.0439 (b)

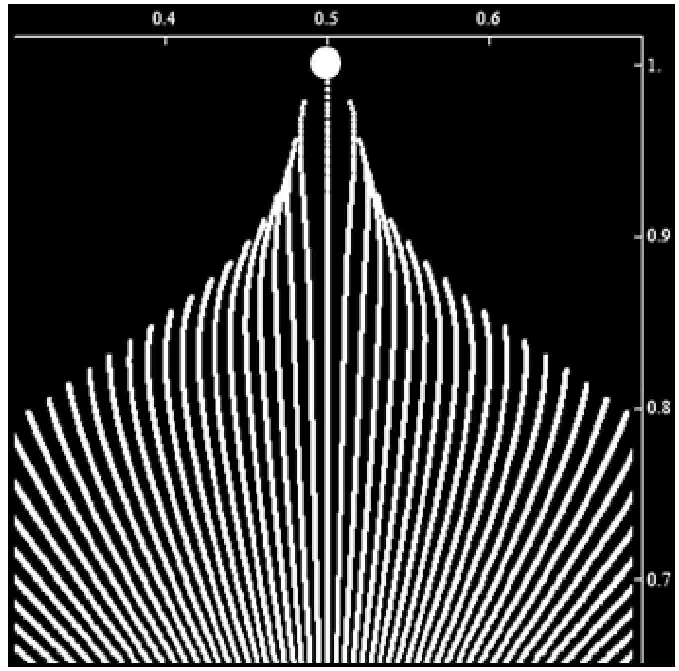

(b)

Fig. 15. The flooding area for nine-point scheme of flooding for κ=1 and τ=0.0277 (a); for κ=1/4 and τ=0.0232 (b)

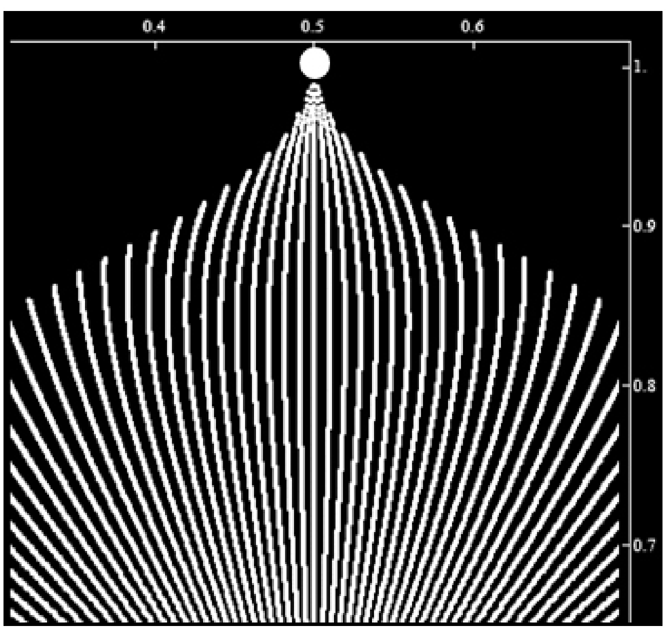

(a)

The Table 1 shows the values of the water breakthrough time into the producing wells τ and the Table 2 - the values of waterflooding coverages K_{cov}, calculated for four of waterflood patterns with different values of κ. Abbreviation VF (viscous fingers) indicates the appearance of the "viscous fingering" for the selected scheme of the flooding.

Therefore, due to violation of the smoothness of the flooding front the count of the values of waterflooding coverages K_{cov} for a given value of κ is not possible. For greater clarity, the columns of Table 2 are supplemented with values, taken from the book by F. Craig [24] for the case of κ=1.

Table 1: The values of dimentionless breakthrough time τ for different values of the mobility κ

Scheme of flooding	Values of the dimensionless breakthrough time $10^4\ \tau$			
	κ=1	κ=1/2	κ=1/3	κ=1/4
Five-point	1152	1017	960	VF
Front row	1820	1500	VF	VF
Seven-point	516	472	452	439
Nine-point	277	252	240	232

Table 2: The values of waterflooding coverages K_{cov} for different values of the mobility κ

Scheme of flooding	Values of the waterflooding coverages K_{cov}				
	[24]	κ=1	κ=1/2	κ=1/3	κ=1/4
Five-point	70%	72%	63%	60%	VF
Front row	58%	57%	47%	VF	VF
Seven-point	73%	75%	68%	65%	63%
Nine-point	55%	53%	48%	46%	44%

IV CONCLUSIONS

The present study is a continuation of [13] and generalizes the previous results to the case of a piston displacement of oil by water, in which the physical properties of different liquids are different. The result of this work is the software system based on the solution of the problem of monitoring the oil-water boundary

The software system provides both graphic data (painting the flooded area), and the values of numerical parameters (the water breakthrough time and the values of waterflooding coverages) for the selected scheme of flooding. The developed software package is a tool for comparative analysis of various schemes of flooding at constant reservoir geophysical parameters: comparison data can be applied in the design of the development of real fields as recommendations to the choice of placement of wells from options defined by the analysis of the geophysical characteristics of the oil-developed area. In this account of physical differences together filterable phase (oil and water) is significantly closer to the realities of the simulated process of oil production.

Features of the program can be expanded in the future with the further development of the scheme of waterflooding: comparative analysis of the data can be refined in the transition to the model of two-phase filtration and expanded assuming variable flow rates injection displacing agent (water). Information on the process of filtering a selected pattern waterflood may also be added to change such forecasts the performance characteristics of the wells and the reservoir as the total production rate, average reservoir pressure and the pressure in the well bottom zone of wells.

REFERENCES

[1] W.T. Koiter, Some general theorems on doubly-periodic and quasi-periodic functions, *Proc. Kon. Ned. Acad. Wt. Amsterdam,* A, Vol. 157, 1959, pp. 120-128.

[2] W.T. Koiter, Stress distribution in an infinite elastic sheet with a doubly-periodic set of holes, in *Boundary problems in differential equations.* Madison: Univ. of Wisconsin Press, 1960, pp. 191-213.

[3] E.I. Grigolyuk and L.A. Filshtinsky, *Perforated Plates and Shells*, Moscow: Nauka, 1970, (in Russian).

[4] N.I. Iokamidis and P.S. Theokaris, Array of periodic curvilinear cracks in an infinite isotropic medium, *Acta Mechanica,* Vol. 28, 1977, pp. 239-254.

[5] A.M. Linkov and V.F. Koshelev, Complex variables BIE and BEM for a plane doubly-periodic system of flaws, *J. Chin. Inst. Eng.,* Vol. 22, 1999, pp. 709-720.

[6] J.D. Eshelby, The continuum theory of lattice defects, in *Progress in Solid State Physics,* vol. 3, F. Seitz and D. Turnbull, Eds. New York: Academic Press, 1956, pp. 79-144.

[7] L.I. Sedov, *Two-dimensional Problems in Hydrodynamics and Aerodynamics*, New York: Wiley, 1965.

[8] V.K. Tkachenko, On vortex lattices, *Soviet Physics, JETF,* Vol. 22, June 1966, pp. 1282-1286, (Engl. transl.).

[9] K.A. O'Neil, On the Hamiltonian dynamics of vortex lattices, *J. Math. Phys,.* Vol. 30, June 1989, pp. 1373–1379.

[10] M.A. Stremler and H. Aref, Motion of three vortices in a periodic parallelogram, *J. Fluid Mech*., Vol. 392, 1999, pp. 101-128.

[11] H.J. Morel-Seytoux, Analytical-numerical method in waterflooding predictions, *SPE Journal*, Vol. 5, September 1965, pp. 247-258.

[12] R.T. Fazlyev, A*real Waterflooding of Oilfields,* Moscow: Nedra, 1979,

[13] V.I. Astafev, P.V. Roters, Simulation of Oil Recovery using the Weierstrass Elliptic Functions, *International Journal of Mechanics*, Vol. 8, 2014, pp. 353-364.

[14] N.I. Akhiezer, *Elements of the Theory of Elliptic Functions,* Providence, RI: American Mathematical Society (translated from Russian as *AMS Translations of Mathematical Monographs. Vol. 79).* 1990.

[15] M. Abramowitz and I.A. Stegun, *Handbook of Mathematical Functions: with Formulas, Graphs and Mathematical Tables,* New York: Dover, 1965.

[16] M. Muskat, *The Flow of Homogeneous Fluids through Porous Media*, New York: McGraw-Hill, 1937.

[17] G. Paul. Willhite, *Waterflooding.* SPE Textbook. Vol. 3. Society of Petroleum Engineers, Richardson, Texas, 1986.

[18] V.I. Astafev, A.E. Kasatkin, P.V. Roters, Elliptic Functions in Modeling of Oil Recovery, *ECMOR XIII – 13th European Conference on the Mathematics of Oil Recovery*. Biarritz, France, 2012. DOI: 10.3997/2214-4609.20143268.

[19] V.I. Astafev, P.V. Roters, *Elliptic Functions in Modeling of Oil Recovery*, Samara, Samara University Publishing, 2014, (in Russian).

[20] V.I. Astafev, A.E. Kasatkin, Elliptic Functions in the Modeling of Waterflooding, *75th EAGE Conference & Exhibition incorporating SPE EUROPEC 2013,* London, UK, 2013. DOI: 10.3997/2214-4609.20130892

[21] V.I. Astafev, A.E. Kasatkin, Modeling and Numerical Calculation of Piston-Like Oil Displacement for Doubly-Periodic Systems of Field Development, *Computational Continuum Mechanics,* Vol. 8, No. 1, 2015, pp. 81-92, (in Russian) DOI: 10.7242/1999-6691/2015.8.1.7

[22] V.I. Astafev, A.E. Kasatkin, Modeling and Numerical Calculation of Piston-like Oil Displacement for Doubly Periodic System of Oil Field Development, *COUPLED PROBLEMS 2015. VI International Conference on Coupled Problems in Science and Engineering*, San Servolo, Venice, Italy, 2015.

[23] V.I. Astafev, *Modeling of Waterflooding Oilfields*, LAMBERT Academic Publishing, 2015, (in Russian).

[24] F.F. Craig, *The Reservoir Engineering Aspects of Waterflooding*. SPE Monograph Series. Vol. 3. Society of Petroleum Engineers, Dallas, 1971.

[25] P.G. Saffman, Viscous Fingering in Hele-Shaw Cells. *Journal of Fluid Mechanics*, Vol. 173, 1986, pp. 73-84.

[26] P. Dapira, J. Glimm, B. Lindquist, and O. McBryan, Polymer Floods: A Case Study of Nonlinear Wave Analysis and of Instability Control in Tertiary Oil Recovery. *SIAM Journal on Applied Mathematics*